DIVISION S-9—SOIL MINERALOGY

Nutrient-Substituted Hydroxyapatites: Synthesis and Characterization

D. C. Golden* and D. W. Ming

ABSTRACT

Incorporation of Mg, S, and plant-essential micronutrients into the structure of synthetic hydroxyapatite (HA) may be advantageous for closed-loop systems, such as will be required on Lunar and Martian outposts, because these apatites can be used as slow-release fertilizers. Our objective was to synthesize HA with Ca, P, Mg, S, Fe, Cu, Mn, Zn, Mo, B, and Cl incorporated into the structure, i.e., nutrient-substituted apatites. Hydroxyapatite, carbonate hydroxyapatite (CHA), nutrient-substituted hydroxyapatite (NHA), and nutrient-substituted carbonate hydroxyapatite (NCHA) were synthesized by precipitating from solution. Chemical and mineralogical analysis of precipitated samples indicated a considerable fraction of the added cations were incorporated into HA, without mineral impurities. Particle size of the HA was in the 1 to 40 nm range, and decreased with increased substitution of nutrient elements. The particle shape of HA was elongated in the c-direction in unsubstituted HA and NHA but more spherical in CHA and NCHA. The substitution of cations and anions in the HA structure was confirmed by the decrease of the d[002] spacing of HA with substitution of ions with an ionic radius less than that of Ca or P. The DTPA-extractable Cu ranged from 8 to 8429 mg kg^{-1}, Zn ranged from 57 to 1279 mg kg^{-1}, Fe from 211 to 2573 mg kg^{-1}, and Mn from 190 to 1719 mg kg^{-1}, depending on the substitution level of each element in HA. Nutrient-substituted HA has the potential to be used as a slow-release fertilizer to supply micronutrients, S, and Mg in addition to Ca and P.

HUMAN EXPLORATION of the solar system (e.g., lunar and Mars outposts) will require astronauts to grow crops in a way that will recycle wastes, supply food, and regenerate water. A RLSS consisting of plants to recycle human wastes while providing food, potable water, and breathable air is in the process of development (Averner, 1989). Past research has investigated a zeoponic system consisting of ammonium- and potassium-loaded zeolite and natural apatite as a possible plant growth substrate in a RLSS (Allen et al., 1995; Ming et al., 1995). In this zeoponic system, the zeolite provides the macronutrients N and K and the apatite provides the Ca, P, Mg, S and some micronutrients. Plants are an integral part of this system as the apatite dissolution is controlled by the removal of the nutrients from the equilibrium solution by plant uptake. Plant growth experiments indicate that the macronutrient requirements for N, K, P, and Ca have been adequately addressed by the zeolite-natural apatite substrate (Allen et al., 1995). However, Mg and some micronutrients need to be supplemented because the natural apatite does not adequately supply all of the plant-essential elements. It is difficult to find naturally occurring apatite with the right solubility and the correct proportion of substituted micronutrients.

An alternative is the use of synthetic apatite. Many elements, including all the plant micronutrients and several macronutrients, can be substituted in apatite, either in anionic (e.g., BO_3^{3-}, MoO_4^{2-}, SO_4^{2-}, and Cl^-) or cationic (e.g., Mg^{2+}, Cu^{2+}, Zn^{2+}, Mn^{2+}, and Fe^{2+}) form (McConnell, 1937; Simpson, 1968; Sommerhauser and Katz-Lehnert, 1985; Ming and Golden, 1995). In addition to the nutrient elements, the substitution of carbonate and fluoride affects the solubility of apatite (Khasawneh and Doll, 1978). Synthetic apatite with many essential elements incorporated into its structure has not been attractive as a fertilizer due to its cost considerations. However, there are some applications where cost may not be prohibitive (e.g., high-value greenhouse crops and agricultural applications in space). A few plant-growth studies have been conducted using synthetic apatite (e.g., Resseler and Werner, 1989) but to our knowledge none have used micronutrient substituted apatite as a soil fertilizer.

The objectives of this study were (i) to synthesize hydroxyapatites and carbonate hydroxyapatite with plant-essential nutrients (Ca, P, Mg, Mo, Cu, Zn, Mn, Fe, B, Cl, and S) incorporated into the structure, (ii) to analytically determine the extent of incorporation into the structure, and (iii) to investigate the suitability of the synthetic apatites as a micronutrient source in addition to providing Ca and P for plant growth.

MATERIALS AND METHODS

Mineral Synthesis and Materials

Hydroxyapatites

The first step in the procedure for synthesis of HA consisted of preparing solutions 1 and 2 (Table 1). The Solution 1 was prepared by mixing 171.74 g of $Ca(NO_3)_2{\cdot}4H_2O$ in 500 mL of 200 g kg^{-1} NH_3 solution. Solution 2 was prepared by dissolving 59.74 g of $(NH_4)_2HPO_4$ in 460 mL of deionized water and then, while stirring vigorously, 39 mL of 200 g kg^{-1} NH_3 solution was slowly added to the reactant mixture. The final pH of Solution

D.C. Golden, Lockheed-Martin Corp., C-23, P.O. Box 58561, Houston, TX 77258-8561 and D.W. Ming, Mail Code SN-4, NASA - Johnson Space Center, Houston, TX 77058. Received 13 Nov. 1997. *Corresponding author (d.c.golden1@jsc.nasa.gov).

Published in Soil Sci. Soc. Am. J. 63:657–664 (1999).

Abbreviations: CHA, carbonate hydroxyapatite; EPMA, electron probe microanalysis; FTIR, Fourier-transform infrared analysis; HA, hydroxyapatite; HRTEM, high-resolution transmission electron microscopy; INAA, instrumental neutron activation analysis; MCD, mean coherently scattering dimension; NCHA, nutrient-substituted carbonate hydroxyapatite; NCPR, North Carolina phosphate rock; NHA, nutrient-substituted hydroxyapatite; RLSS, regenerative life support system; SEM, scanning electron microscopy; STEM, scanning transmission electron microscope; TEM, transmission electron microscopy; and XRD, X-ray diffraction analysis

Table 1. Compositions of solutions used for synthesis of hydroxyapatites.

Chemical	Mineral†			
	HA	CHA	NHA	NCHA
			Solution 1	
			g/500 mL	
$Ca(NO_3)_2{\cdot}4H_2O$	171.74	171.74	141.52	141.52
			Solution 2	
			g/500 mL	
$(NH_4)_2HPO_4$	59.74	50.0	43.32	43.32
$(NH_4)Cl$	–	–	1.011	1.011
H_3BO_3	–	–	6.0×10^{-2}	0.779
$(NH_4)_6Mo_7O_{24}{\cdot}4H_2O$	–	–	9.8×10^{-4}	9.8×10^{-4}
$(NH_4)_2SO_4$	–	–	2.497	2.497
$(NH_4)_2CO_3$	–	11.93	–	11.93
			Solution 3	
			g/20 mL	
$Fe(NO_3)_2{\cdot}6H_2O$	–	–	3.627	4.942‡
$MnSO_4{\cdot}H_2O$	–	–	0.5408	0.5408
$Zn(NO_3)_2$	–	–	0.5652	0.5652
$Cu(NO_3)_2{\cdot}2.5H_2O$	–	–	0.1464	0.1464
$Mg(NO_3)_2$	–	–	13.499	13.499

† HA = hydroxyapatite, CHA = carbonate HA, NHA = nutrient substituted HA, NCHA = nutrient-substituted CHA.
‡ Fe was weighed as $Fe(NH_4)_2(SO_4){\cdot}6H_2O$ for this sample.

2 was about 12. Solution 2 was added to Solution 1, while vigorously stirring the mixture. The resulting precipitate was aged for 24 h at room temperature. After this aging, 3 L of deionized water was added to wash the precipitate, which was then stirred and allowed to settle. The supernatant was decanted, and the precipitate was washed with deionized water three times or until excess NH_4NO_3 was removed. The washed precipitate was filtered using Whatman no. 42 filter paper and a Buchner funnel and then dried in an oven at 70°C.

Carbonate Hydroxyapatite

Solutions used for synthesis of CHA were similar to those for synthesis of HA except that $(NH_4)_2CO_3$ was included in Solution 2 (Table 1). Solution 2 was added to Solution 1 while stirring. The mixture was stirred for 5 min. The aging, filtration, washing, drying, and heating procedures were similar to those described for HA. In the rare event a carbonate (e.g., calcite) precipitate was confirmed by XRD analysis, the precipitate was treated with ammonium phosphate buffer (pH 5) to bring the final pH of the suspension to about 6. The treated precipitate was washed with deionized water to remove excess buffer, and the final residue was filtered and dried as for HA.

Nutrient-Substituted Hydroxyapatites

Synthesis of NHA was similar to that of HA except that a third solution (Solution 3) in addition to Solutions 1 and 2 was used for synthesis of NHA (Table 1). Solution 2 contained P and the anionic substituents, while Solution 3 was made up of cationic substituents. The substitution levels of elements were changed by varying the amount of substituent in the reaction mixture while keeping the total cations to total anions mole ratio approximately constant. Solution 3 was added to Solution 2 while vigorously stirring and then the whole mixture of Solutions 2 and 3 were immediately added to Solution 1. Stirring was continued for 5 min. The aging, filtration, washing, drying, and heating procedures were similar to those described for HA. In selected preparations, reducing conditions were maintained in the reaction mixture to prevent the oxidation of Fe^{2+} to Fe^{3+} by adding L-ascorbic acid and having a stream of N_2 flow through the system. The incorporation of elements could be varied within a given HA by varying the ratio of the initial reagents used in the synthesis.

Another series of NHAs with just a single nutrient substituted into hydroxyapatite was prepared in a similar fashion to the above procedure. The added nutrient was ~10 to 11 mole percent of the Ca (in the case of cations) or P (in the case of anions). The nutrient was incorporated into Solution 2 if it was an anion and into Solution 3 if it was a cation. These precipitates were analyzed by XRD and IR to determine if the Mg, S, and micronutrients were incorporated into the hydroxyapatite structure.

Nutrient-Substituted Carbonate Hydroxyapatites

Solutions used for synthesis of NCHA were similar to those used to synthesize NHA except that $(NH_4)_2CO_3$ was included in the Solution 2 (Table 1). Solution 3 was added to Solution 2 while vigorously stirring and then the mixture of Solutions 2 and 3 was immediately added to Solution 1. Stirring was continued for 5 min. The aging, filtration, washing, drying, and heating procedures were similar to those described for HA.

Natural Apatite

North Carolina phosphate rock (NCPR) was obtained from the Texas Gulf Corp. and the as-received samples were sieve fractionated to obtain <54 μm fraction (fine fraction). Calcium carbonate in the NCPR fine fraction was removed by treating with 0.2 M ammonium phosphate buffered to pH 5. The NCPR was allowed to stand overnight in the buffer with a solid-to-solution ratio of 1:5. The chemical analysis of the NCPR is given in Table 2. The NCPR is widely used as a direct application P-fertilizer (White et al., 1989). Therefore it was used as a standard for comparison with the synthetic hydroxyapatites.

Chemical Analyses

Electron Probe Microanalysis

Synthetic hydroxyapatite powder was pressed into smooth-surface pellets by using a die and a hydraulic press. The pellet was mounted on a circular petrographic glass slide using epoxy resin and carbon-coated prior to electron probe microanalysis, which was performed at 15 kV with the beam in raster mode (3×3 μm) on a Cameca Camebax microprobe (Trymbull, CT). Polished National Institute of Standards and Technology mineral standards and NCPR pellets prepared in a similar fashion to those of synthetic HAs were used as standards and the data was reduced with the Cameca ZAF reduction program.

Atomic Absorption and Colorimetric Analyses

Synthetic HA samples (0.2 g) were dissolved in a hot conc. $HCl–HNO_3$ mixture. Resulting solutions were diluted and analyzed for Ca, Zn, Cu, Mg, Na, Fe, Mn and K by atomic absorption spectrometry. Phosphorus was measured colorimetrically by using a phosphomolybdate blue method (Olson and Watanabe, 1957).

Instrumental Neutron Activation Analysis

For INAA, the samples, standards, and a sample of NCPR were encapsulated in pure SiO_2 glass tubes and irradiated at the Texas A&M Univ. reactor facility for 2 h at a flux of 2.8×10^{12} n cm^{-2} s^{-1}. A series of three counts was performed at 12 and 24 h, and 1 wk after irradiation in order to obtain data

Table 2. Chemical analysis of nutrient-substituted hydroxyapatite and their DTPA extractable elements.

Mineral†	Elemental concentration										Substitute anion	Substitute cation	DTPA extractable				
	Ca	P	B	Fe	S	Mo	Zn	Mg	Mn	Cu			Fe	Zn	Mg	Mn	Cu
	g kg^{-1}										mole %		mg kg^{-1}				
HA	374	174															
CHA	365	161															
NHA	327	164	0.3	11.0	3.9	0.0	0.6	12.7	2.4	0.1	2.77	8.70	501	57	1541	190	8
NCHA	332	154	1.1	6.9	2.1	0.0	0.4	12.1	2.4	0.1	3.16	7.52	211	78	2588	114	24
MgHA(1)	345	174						17.3			0.00	7.63			4975		
MgHA(2)	342	175						20.5			0.00	8.99			5299		
CuHA(1)	358	170								15.4	0.00	2.65					4072
CuHA(2)	352	170								20.7	0.00	3.58					8429
MnHA(1)	339	174			1.8				49.2		1.00	9.58				1719	
MnHA(2)	333	163			9.6				49.6		5.40	9.81				1719	
FeHA(1)	310	156		50.8	4.7						2.83	10.54	2573				
FeHA(2)	346	180		49.9							0.00	9.37	2476				
ZnHA(1)	354	169					18.9				0.00	3.18		741			
ZnHA(2)	344	170					34.8				0.00	5.84		1279			
MoHA	373	166				20.7					3.84	0.00					
SHA	381	168			8.8						4.78	0.00					
BHA	373	154	6.9								11.42	0.00					
NCPR	318	124	0.1	3.6	6.1		3.6	2.8	0.0	0.0							

† Abbreviations: HA = hydroxyapatite; CHA = carbonate hydroxyapatite; NHA = nutrient-substituted hydroxyapatite; MHA = M-substituted hydroxyapatite; where, M = Mg, Cu, Mn, Fe, Zn, Mo, S or B, NCHA = nutrient-substituted CHA; and NCPR = North Carolina phosphate rock. Numeral in parentheses identifies the batch number.

for nuclides with differing half-lives. Calcium, Mn, Fe, Cu, and Zn were analyzed by INAA; but, Mo was below detection limits except for the single-nutrient-substituted HA. Details of the NASA Johnson Space Center INAA data reduction procedure are given in Mittlefehldt and Lindstrom (1993) and references therein. In addition, Cu data were corrected for interference from positrons produced by pair production from ^{24}Na gamma rays using data from Cu-free samples. Positrons from pair production from other nuclides was insignificant relative to the positrons for ^{64}Cu.

Citric Acid Extraction for Phosphorus

Samples of hydroxyapatite (0.1 g) were shaken with 10 mL of 20 g kg^{-1} citric acid solution in an environmental orbital shaker at 25°C for 1 h (AOAC, 1960; Syers and Mackay, 1980). After shaking, samples were centrifuged at 15 000 rpm for 10 min. and an aliquot of the supernatant was used to determine extractable P. Phosphorus was measured colorimetrically as above.

Equilibrium Solubility

To determine the Ca and P concentration in equilibrium with HA in aqueous solution, quantities of HA containing approximately 250 mg P (calculated from the total g kg^{-1} P of HA) were placed in 250 mL Erlenmeyer flasks with 100 mL of deionized water. Flasks were covered with Parafilm and gently shaken in an environmental orbital shaker for 60 d. Gas exchange with the atmosphere was maintained through a pinhole in the Parafilm. Subsamples were drawn at 7-d intervals and analyzed for Ca and P to ascertain the attainment of equilibrium. By 6 to 7 wk the solution concentrations had stabilized. At the end of the 60 d, the samples were centrifuged and the supernatants were filtered and analyzed for electrical conductivity (EC), pH, Ca, P, Na, and Mg. Ionic strengths (μ) were calculated using the empirical relation between EC and μ reported by Griffin and Jurinak (1973), cited by Lindsay (1979) as follows:

$$\mu = 0.013\ (EC) \qquad [1]$$

where μ is the ionic strength based on concentration expressed in moles L^{-1} and EC is the electrical conductivity expressed in dS m^{-1} at 25°C.

Activities of ions were calculated using the Davies equation (Davies, 1962) as follows:

$$\log \gamma_i = -AZ_i^2 \{[\mu^{1/2}/(1 + \mu^{1/2})] - 0.3\mu\} \qquad [2]$$

where $A = 0.509$ for water at 25°C and Z_i is the charge on the ion. The values of $pH_2PO_4 + 1/2$ pCa and pH $-$ 1/2 pCa were calculated for the equilibrated solutions and plotted along with the calculated solubility values obtained using thermodynamic data for HA (Chien and Black, 1976).

Micronutrient Availability

The availability of micronutrients to plants was tested by using the DTPA extraction procedure of Lindsay and Norwell (1978), whereby 20 mL of the DTPA extraction solution was added to 0.1 g of synthetic HA placed in a 125 mL conical flask. The conical flasks were covered with parafilm and shaken in a horizontal shaker at 120 cycles min^{-1}. After 2 h of shaking, the solutions were filtered through Whatman no. 42 filter paper. The filtrates were analyzed for Fe, Zn, Cu, Mn, and Mg by atomic absorption spectrometry using the appropriate standards in a matching matrix. Extractability of anionic micronutrients was not tested.

Mineralogical Analyses

X-ray Diffraction of Synthetic Hydroxyapatites

Freeze-dried powders of synthetic HAs were mounted on cavities carved on glass slides and X-rayed using CuKα radiation on a Scintag XDS 2000 X-ray diffractometer (Cupertino, CA) equipped with a graphite monochromator. Ten to 60 degree two-theta scans were performed for all the samples. In addition selected peaks were slow scanned (0.25° 2θ per minute) for the mean coherently scattering dimension (MCD) determination. The MCD[hkl] perpendicular to a given lattice plane [hkl] was calculated using the broadening of X-ray peak profile corresponding to d[hkl]-spacing assuming no strain was present. The residual peak broadening after subtracting the peak width due to instrumental effects can be related to the crystallite size by the Scherrer equation (Klug and Alexander, 1974; Zussman, 1977).

The substitution of cations (Mg, Zn, etc.) into the hydroxyapatite structure was confirmed by measuring the shift of the

d[002] spacings by X-ray diffraction compared to synthetic HA. According to the Vegard's rule for isomorphic substitution, the X-ray d-spacing of a member of an isomorphous series is

$$d[hkl]_0 - d[hkl]_x = xK \quad [3]$$

where x is the mole fraction of substitution, $d[hkl]_0$ is the hkl d-spacing for synthetic hydroxyapatite, $d[hkl]_x$ is the hkl d-spacing for the x mole % nutrient-substituted hydroxyapatite and K is a constant that depends on the ionic radius (R_m) of the substituted nutrient (M). For a first approximation, the ionic radius R_m is assumed to be linearly related to K (i.e., $K = kR_m$, where k is a constant). Then for any cation M substituting for Ca in hydroxyapatite,

$$d[hkl]_0 - d[hkl]_x = kx(R_m) \quad [4]$$

where, R_m is the radius of the substituting cation M.

Therefore, Eq. [4] may be rewritten as

$$d[hkl]_x = d[hkl]_0 - kx(R_m) \quad [5]$$

A plot of $d[hkl]_x$ versus xR_m should be a straight line with a negative slope and $d[hkl]_0$ as the intercept. For single micronutrient substituted HA samples, the d[002] reflection was selected for determining substitution, because it was free from overlapping peaks. The d[002] peak was scanned at 0.25°/min three times for each sample. A quartz calibration standard was run between each scan.

Fourier Transform Infrared Spectroscopy

The FTIR spectroscopy was performed on 2-mm diameter KBr pellets containing approximately 3 g kg^{-1} HA using a BIORAD Fourier Transform Infrared Spectroscopy instrument. Weighed samples were ground to <50 μm and homogenized with KBr in an agate mortar. Pelletization was performed by placing the ground sample and KBr mix in a die and applying a pressure of 5 Mg for 1 min. The IR scans were performed from wavenumbers of 500 to 4000 cm^{-1}.

Transmission Electron Microscopy

The HA was dispersed in distilled water (100 mg L^{-1}) and a drop of the suspension was evaporated on a holey-carbon film. The dried sample was sputter-coated with a 20-nm thick C layer prior to examination with a JEOL JEM-2000 FX scanning transmission electron microscope (STEM). High resolution transmission electron microscopy (HRTEM) measurements were used to verify the particle size measured by XRD.

RESULTS

Synthesis Procedure and Composition

The NHAs were gray to light red in color, depending on the oxidation state of the substituting Fe. Samples prepared under reducing conditions were gray, indicating reduced Fe. When the precipitation was conducted in the presence of air, a light-red-colored product was obtained. In all cases the samples were homogeneous in color to the naked eye. Total chemical analysis performed by a combination of electron microprobe, INAA, and wet chemical methods indicated incorporation of the added elements into the HA structure (Table 2). Incorporation of Mo was not determined except for the MoHA sample (Table 2) due to the limitations of the analytical methods to measure Mo. Single-nutrient substitution in hydroxyapatite to study the X-ray line shifts was done at a higher substitution level (e.g., 3–11 mole %) than in multiple nutrient substituted hydroxyapatites (Table 2).

X-ray Diffraction Analysis

The XRD patterns of synthetic HA, NHA, CHA, and NCHA are shown in Fig. 1. The NCHA has broader XRD peaks than CHA and HA. Because the substitution of several elements at low levels were done simultaneously, correlation of the X-ray line shifts due to each substituent was difficult to detect except in the single-nutrient-substituted HA where measurable shifts in XRD spacings due to higher substitution were observed. Apart from the differences in peak widths and minor peak shifts, all of the synthetic apatites have similar XRD patterns and appear to contain no XRD-detectable mineral impurities. However, in certain high-carbonate synthetic hydroxyapatites (not shown) a small amount of calcite precipitated along with the hydroxyapatite. Also, in the Fe-containing hydroxyapatites formed under oxidizing conditions, the red color may indicate the precipitation of Fe^{3+} oxide in trace quantities; however, no Fe-oxides were detected by XRD analysis.

Because multiple nutrient-substituted HAs were not suitable for XRD-line shift determination, d[002] spacings of single nutrient-substituted HAs with high substitution levels specifically prepared for this purpose were examined. All the HAs with cations incorporated into them exhibited shifts of [002] line to shorter d-spacings suggesting substitution in the HA structure. This would be expected if substitution has occurred since the ionic radii of all the cations added were smaller than 0.99 Å of Ca (e.g., Mg = 0.65 Å, Mn = 0.80 Å, Fe^{2+} = 0.76 Å, Fe^{3+} = 0.64 Å, Cu = 0.87 Å, and Zn = 0.88 Å). The

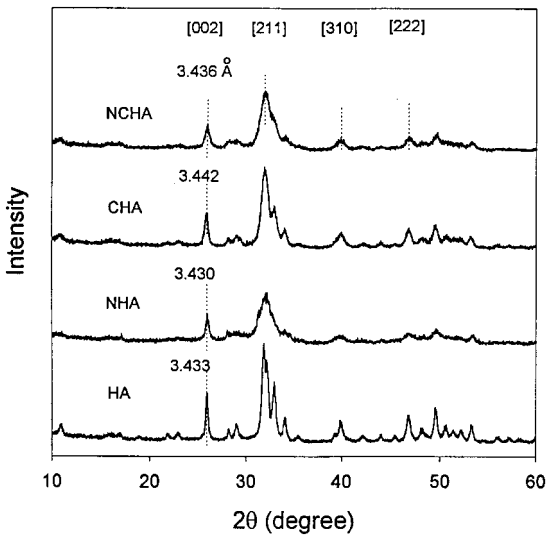

Fig. 1. X-ray diffraction patterns (CuKα radiation) of hydroxyapatite (HA); nutrient-substituted hydroxyapatite (NHA); carbonate hydroxyapatite (CHA); and nutrient-substituted carbonate hydroxyapatite (NCHA). Broad XRD peaks suggest that nutrient and carbonate substitution reduces hydroxyapatite crystallinity.

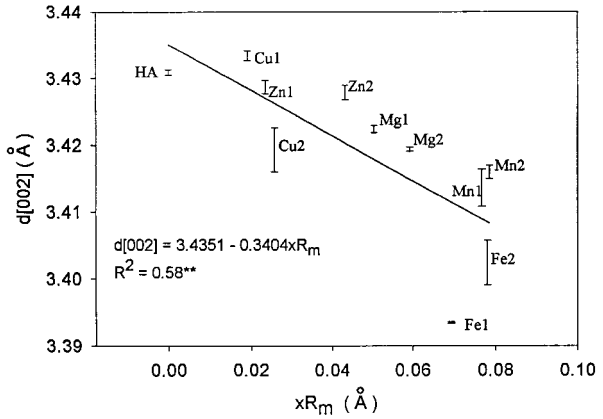

Fig. 2. Plot of d[002] spacing vs. xR_m for the single-nutrient substituted hydroxyapatite (HA). Where x is the substitution mole percent of a given element and R_m is the ionic radius. In the data labels, the chemical symbol represents the substituent ion, HA represents unsubstituted hydroxyapatite and the end numeral refers to the batch number 1 or 2. Substitution of elements with smaller R_m caused d[002] spacing to decrease. Error bars represent 2σ.

plot of d[002] vs. xR_m is linear with a negative slope (Fig. 2) confirming that the cations were substituted for Ca in the hydroxyapatite structure.

Fourier Transform Infrared Spectroscopy

The infrared spectra of HAs are sensitive to their composition (e.g., vibrations originating from OH, CO_3, and PO_4 structural groups). The IR spectra of synthetic hydroxyapatites (Fig. 3) qualitatively revealed the presence of the above structural groups and were useful in studying the relative amount of the substituting anions such as CO_3. Carbonate absorptions are at or near 1453, 1428 ($CO_3 - \nu_3$) and 865 cm^{-1} ($CO_3 - \nu_2$). The vibrations

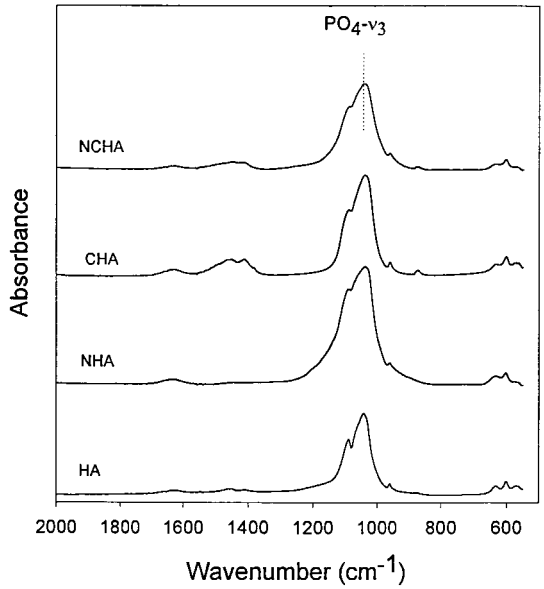

Fig. 3. FTIR spectra of hydroxyapatites: Hydroxyapatite (HA); Nutrient-substituted hydroxyapatite (NHA); Carbonate hydroxyapatite (CHA); and Nutrient-substituted carbonate hydroxyapatite (NCHA). Line broadening with substitution is evident in IR spectra of the apatites as indicated by the merging of the absorption bands.

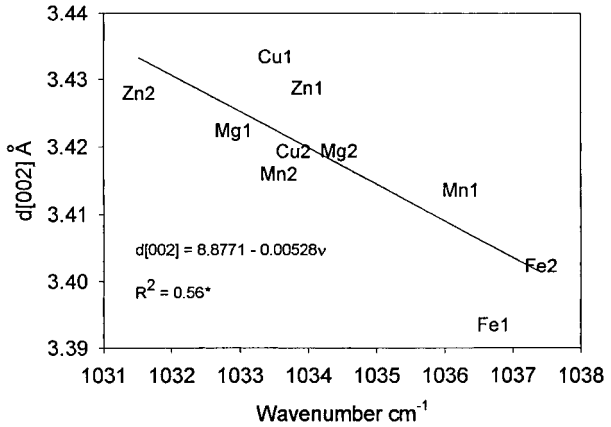

Fig. 4. A plot of the most intense $PO_4 - \nu_3$ IR absorption peak position versus the XRD d[002] spacing. As the d[002] spacing decreased the wavenumber for the $PO_4 - \nu_3$ absorption peak decreased. Data labels are same as in Figure 2.

at 1096 and 1036 ($PO_4 - \nu_3$) are best resolved when the carbonate substitution is the least. Substitution of carbonate or micronutrients in HA appears to cause broadening of IR absorption bands (Fig. 3). The $PO_4 - \nu_3$ band with highest absorption appeared to increase in wavenumber with decrease in d[002] (Fig. 4).

Transmission Electron Microscopy

High-resolution transmission electron microscopy (HRTEM) was used to observe the size, morphology, and lattice fringes of HA (not shown), CHA (Fig. 5a), and NCHA (Fig. 5b). In addition, no crystalline impurities were detected by measuring the lattice spacings and chemical composition (energy dispersive X-ray analysis). The domain size (thickness of regular-stacked atomic layers) as observed by HRTEM and the physical particle sizes as measured by XRD were similar (10–20 nm) for all samples. Individual particles of CHA were equant and 10 to 20 nm in diameter. The morphology of the NCHA was similar to that of CHA. HA and NHA crystals (not shown) were elongated and CHA and NCHA crystals were rounded as suggested by the MCD[002]/MCD[222] ratio close to 1 (not shown). Assuming different solubilities for different crystal faces, crystal shape should influence the solubility of the hydroxyapatite particles. HRTEM image of a NCHA particle (inset of Fig. 5b) along the direction of the hexagonal tunnels showed (100) and (010) d-spacings of approximately 0.81 nm. HRTEM images of NCPR showed cemented, equant, 20 to 30 nm crystallites in random orientation (not shown) and were slightly larger than the synthetic HA crystallites.

Equilibrium Studies and Solubility in Citric Acid

Concentrations of ions in an aqueous solution (deionized water) after a 60-d contact with synthetic HA powders were used to calculate the pH_2PO_4 and pCa. The points in the plot for the synthetic minerals fell near or below the calculated HA solubility line (line marked HA in Fig. 6). Many synthetic HA points were still below the HA line suggesting super saturation with respect to

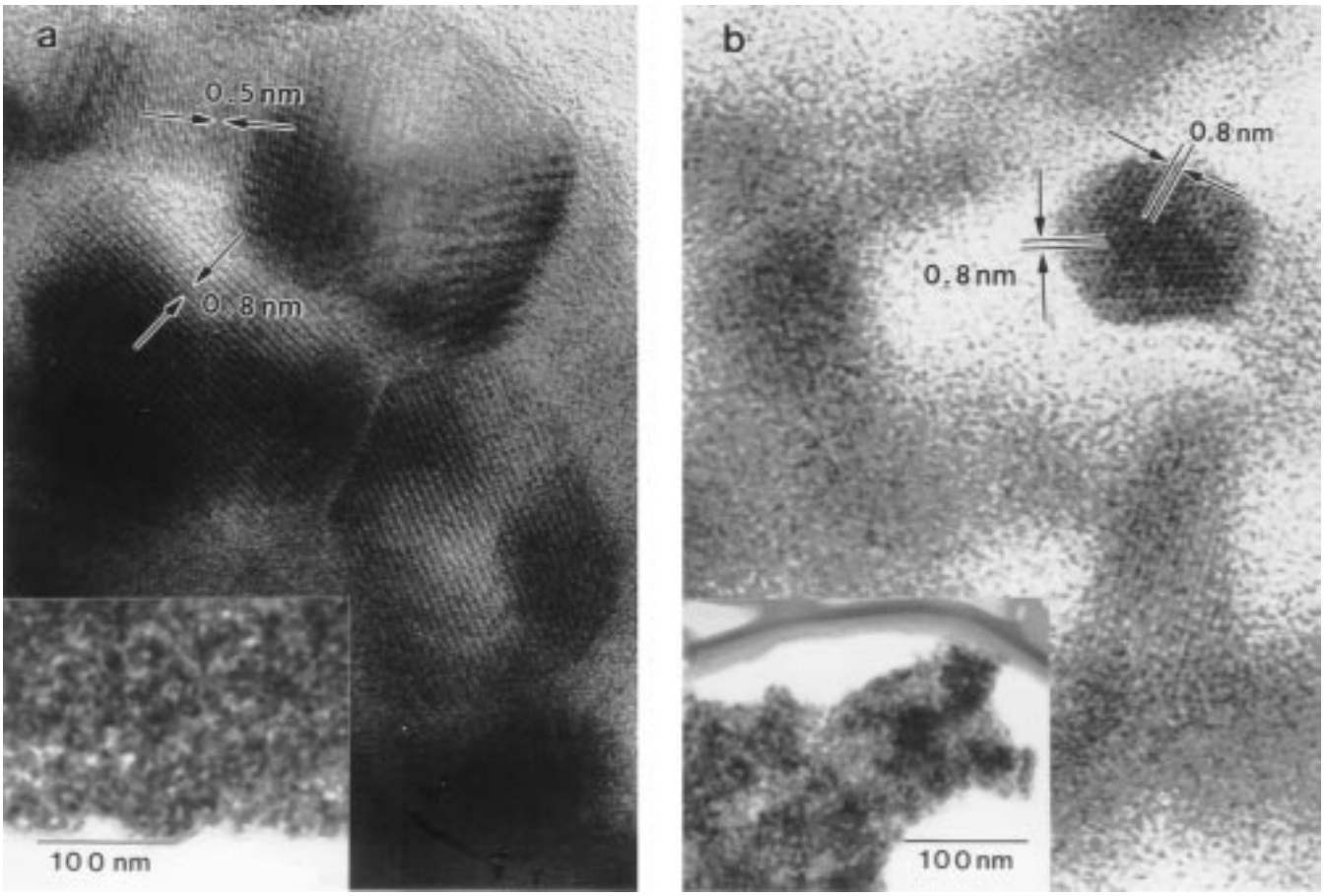

Fig. 5. High resolution transmission electron micrographs (HRTEM) of: (a) carbonate hydroxyapatite (CHA); and (b) nutrient-substituted carbonate hydroxyapatite (NCHA). Note the size of coherent scattering domains in CHA (~25 nm) and that of the nutrient-substituted carbonate hydroxyapatite (~15nm). Coherent scattering domain size for HA was ~30 nm (not shown). Insets show the particles at low magnification.

HA but the data points in general were moving towards the equilibrium with time (data not shown). NCPR data points fell within the central region of the data point cluster. NCPR, a carbonate-substituted fluorapatite, would be expected to be above the HA line. The fact that out of the two data points for NCPR one point fell below the HA line suggests that the system was still approaching equilibrium even after 60 d. Total P available for plant growth (citric acid extractable P) was nearly 100% for HA and CHA (Table 3). Available P was about 20% lower for NCHA and 25% lower for HA.

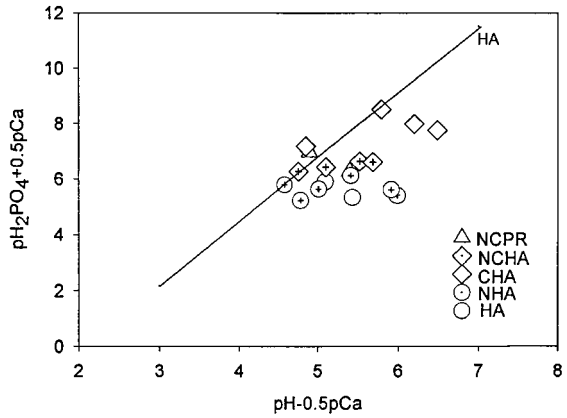

Fig. 6. Solubility isotherms of hydroxyapatite. Points in the scatter plot correspond to the activities of ions in solution in contact with synthetic hydroxyapatites (HA); nutrient substituted hydroxyapatites (NHA); carbonate hydroxyapatite (CHA); nutrient-substituted carbonate hydroxyapatite (NCHA); and North Carolina phosphate rock (NCPR). The solid line is for pure hydroxyapatite calculated from thermodynamic data (Chien and Black, 1976; Khasawneh and Doll, 1978).

Micronutrient Availability

To assess the micronutrient release when applied to the soil, DTPA extractable micronutrients were determined for NHAs with varying substitution levels (Table 2). We found that higher substitution levels resulted in higher DTPA extractable micronutrient (e.g., Fe, Zn, Cu, Mg and Mn). The relationship between the DTPA

Table 3. Availability of P in hydroxyapatite and North Carolina phosphate rock (NCPR) by 2% citric acid extraction (CiP).

Sample†	Total P	CiP	(CiP/Total P) × 100
	g kg^{-1}		
HA	175	174.2	99.5
CHA	175	174.6	99.7
NHA	174.5	131.8	75.5
NCHA	175.1	139.9	79.89
NCPR	133	58.2	43.75

† HA = hydroxyapatite, CHA = carbonate hydroxyapatite, NHA = nutrient-substituted hydroxyapatites, and NCHA = nutrient-substituted carbonate hydroxyapatite.

extractable elements as linear regression equations are shown below,

$$\text{DTPA}-\text{Fe} = 498.6(x) \quad [R^2 = 0.99,\ P < 0.01] \quad [6]$$

$$\text{DTPA}-\text{Zn} = 373.4(x) \quad [R^2 = 0.99,\ P < 0.01] \quad [7]$$

$$\text{DTPA}-\text{Mg} = 2367.3(x) \quad [R^2 = 0.81,\ P < 0.05] \quad [8]$$

$$\text{DTPA}-\text{Mn} = 348.64(x) \quad [R^2 = 0.99,\ P < 0.01] \quad [9]$$

$$\text{DTPA}-\text{Cu} = 3563.2(x) \quad [R^2 = 0.91,\ P < 0.05] \quad [10]$$

where x is the weight percent substitution of a given element in HA. Therefore, the micronutrient release is controlled by the substitution level in NHA and can be predicted knowing the substitution level of a given micronutrient element.

DISCUSSION

Synthesis of hydroxyapatite involves mixing two solutions; Solution 1 contained Ca in the form of $Ca(NO_3)_2 \cdot 4H_2O$, and Solution 2 contained PO_4 as $(NH_4)_2HPO_4$. In preparing nutrient-substituted or carbonate-substituted HAs, the substituent elements, which were in anionic form (Cl^-, BO_3^{3-}, MoO_4^{2-}, and SO_4^{2-}), were incorporated into Solution 2. The elements Fe, Mn, Zn, Cu, and Mg were added as bivalent cations. These cationic elements were mixed independently from Solution 1 and 2 to prevent precipitation of metal hydroxides prior to mixing, because Solutions 1 and 2 were maintained at high pH. In the synthesis procedure, quick mixing of Solution 3 with Solution 2 and its immediate transfer to Solution 1 is important in order to prevent precipitation of products other than HA.

No attempt was taken to determine the upper limit of nutrient substitution. Regardless of the level of substitution, no discrete phases containing nutrients other than the expected hydroxyapatites were observed by EMPA, HRTEM, TEM, or XRD analyses. Some calcite precipitated in the very high carbonate substitution levels and those samples were not included in this study. A trace of carbonate is suspected when the synthetic product in aqueous suspension exhibits a pH of about 8.2. The final precipitate may be washed in 0.1 M ammonium phosphate buffer (pH = 5) to remove the carbonate if this occurs.

For the multiple nutrient substituted hydroxyapatites, substitution was achieved at the mg kg^{-1} level. At such a level, the XRD unit cell parameter shifts are not large enough to exceed the measurement error. Therefore, a special set of synthetic hydroxyapatites was prepared by incorporating enough micronutrient in the reactant mixture to form ~10 to 11 mole percent substituted HA if all the reactants had reacted completely. The actual substitution was near the expected value (10–11 mole %) for MnHA, FeHA, MgHA and BHA (Table 2). However, for MoHA, SHA, ZnHA, and CuHA the substitution level was much lower than expected. The latter elements may have attained the maximum limiting substitution under the conditions of the synthesis or else the conditions were not right for the completion of the reaction.

Citric acid solubility is generally used to evaluate the available fertilizer P (Caro and Hill, 1956). Among the factors contributing to the citric acid solubility are particle size and the carbonate substitution (Khasawneh and Doll, 1978).

The products from all the syntheses were investigated for shifts in d-spacings. The [002] XRD peak (Fig. 1) was specially suited for this purpose as it was free of overlap from adjoining peaks and also did not show excessive line broadening which requires a correction of line position for particle size effects (Schulze, 1982). The plot of d[002] vs. xR_m was a straight line (Fig. 2) with a negative slope and an intercept of 3.4351 Å which is very close to d[002] for HA. The data for the cationic single nutrient substituted HA is consistent with the fact that all the nutrients substitute into the HA structure. The shift of the IR $PO_4 - \nu_3$ absorption band to higher wave numbers with shortening of d[002] with increased substitution is consistent with an increased bond strength of P − O when the short ionic radius cations are substituted for Ca in the HA structure. Therefore, the shift in $PO_4 - \nu_3$ band suggests that there is structural substitution of nutrients. The large scatter ($R^2 = 0.56$) in this plot is due to the influence of factors other than substitution of a given element on the $PO_4 - \nu_3$ IR frequency (e.g., particle size, presence of more than one substituent, etc.). HRTEM can detect minor phases if present even in a nanometer scale. Many samples were examined for the presence of such phases using HRTEM and no phases other than HA were observed. Therefore, the micronutrient contents shown in the total chemical analysis were assumed to be structurally substituted. MCDs of the HA particles measured by X-ray line broadening and HRTEM observations (not shown) were approximately similar, suggesting that the HA crystals consisted of uniformly stacked atomic layers free of lattice defects.

Nutrient-substituted carbonate hydroxyapatite was more soluble than NHA in citric acid. This is consistent with carbonate substitution increasing the solubility of apatites as reported by Khasawneh and Doll (1978), but the citric acid extractable P in HA and CHA was close to the total P content. NCPR, a natural carbonate fluorapatite, had the least citric acid soluble P (58.2 g kg^{-1}) and the CHA had the highest citric acid soluble P (174.6 g kg^{-1}) (Table 3). Hydroxyapatite is generally more soluble than fluorapatite (Lindsay and Moreno, 1960). The absence of fluoride and the reduced particle size of CHA makes it more soluble compared to NCPR. NCPR contains approximately 16 g kg^{-1} silica as SiO_2 (data not shown), which may act as a cementing agent if present as a separate phase or may affect the solubility of apatites if substituted in the structure. The lower citrate extractable P for NCPR may be due to the presence of Si, F and particle size effects.

The DTPA extractable micronutrients Fe, Zn, Mn, Cu and the secondary element Mg were linearly related to the substitution level. Therefore, the amount of nutrient substituted fertilizer in a given fertilizer mix can be adjusted to a required DTPA-micronutrient level using these relationships.

CONCLUSIONS

This study demonstrates that a nutrient-substituted hydroxyapatite of a favorable composition and solubility characteristics can be synthesized for zeoponic and other special agricultural applications. The ratio of the nutrients in the HA structure (especially the micronutrients) can be adjusted to suit crop requirements by adjusting the ratio of the components in the synthesis mixture. These nutrient-enriched HAs may provide plant requirements of P, Ca, S, Mg, and micronutrients under suitable dissolution conditions. Citric acid extractions indicate a 132 to 175 g kg^{-1} P extractable P in these synthetic HAs. Availability of P can be adjusted by varying the CO_3 content, particle size, and by other substitute elements. Nutrient substitution apparently reduced citric acid extractable P by about 20% from that of CHA.

Although in this experiment the nutrients were incorporated to balance plant nutrient requirements, adjustments in substitution may become necessary depending on the crop. The synthetic hydroxyapatites are intended as fertilizers for artificial plant growth systems, e.g., zeoponics and hydroponics, where there is no competing P-fixation due to substrate constituents. In an NHA, Ca, P and the substituted nutrient release is controlled by the solubility of the HA. The availability of the micronutrients (DTPA extraction) was proportional to their substitution level. The ability to control the solubility by changing the substituent elements and environmental conditions, and the availability of micronutrients by changing the substitution level is a distinct advantage in synthetic HA based growth media. Experiments are currently being conducted to determine the performance of synthetic HA as a component in zeoponic substrates for cropping systems intended for space applications. Zeoponics promises to be an efficient food production and waste-recycling system (Ming et al., 1995).

ACKNOWLEDGMENTS

The authors wish to thank Lindsay P. Keller for his help in HRTEM, D.W. Mittlefehldt and R.R. Martinez for INAA analysis, C. Galindo, Jr. and J.E. Gruener for laboratory support and Dave Moore for his help in FTIR. The manuscript was benefited from the comments of three anonymous reviewers and the associate editor Dr. David Laird.

REFERENCES

Allen, E.R., D.W. Ming, L.R. Hossner, D.L. Henninger, and C. Galindo. 1995. Growth and nutrient uptake of wheat in clinoptilolite-phosphate rock substrates. Agron. J. 87:1052–1059.

Association of Official Analytical Chemists. 1960. Official methods of analysis. 9th ed. Sec. 2.031b. Assoc. of Official Analytical Chemists, Washington, DC.

Averner, M.M. 1989. Controlled ecological life support system: p. 145–153. *In* D.W. Ming and D.L. Henninger (ed.) Lunar base agriculture: soils for plant growth. ASA, Madison, WI.

Caro, J.H., and W.L. Hill. 1956. Characteristics and fertilizer value of phosphate rock from different fields. J. Agric. Food Chem. 4:684–687.

Chien, S.H., and C.A. Black. 1976. Free energy of formation of carbonate apatite in some phosphate rocks. Soil Sci. Soc. Am. J. 40: 234–239.

Davies, C.W. 1962. Ion associations. Butterworths, London.

Griffin, R.A., and J. Jurinak. 1973. Estimation of activity coefficients from the electrical conductivity of natural aquatic systems and soil extracts. Soil Sci. 116:26–30.

Khasawneh, F.E., and E.C. Doll. 1978. The use of phosphate rock for direct application to soils. Adv. Agron. 30:159–206.

Klug, H.P., and L.E. Alexander. 1974. X-ray diffraction procedure for polycrystalline and amorphous materials. 2nd ed., John Wiley and Sons, New York.

Lindsay, W.L. 1979. Chemical equilibria in soils. John Wiley and Sons, New York.

Lindsay, W.L., and E.C. Moreno. 1960. Phosphate phase equilibria in soils. Soil Sci. Soc. Am. Proc. 24:177–182.

Lindsay, W.L., and W.A. Norwell. 1978. Development of a DTPA soil test for zinc, iron, manganese and copper. Soil Sci. Soc. Am. J. 42:421–428.

McConnell, D. 1937. The substitution of SiO_4 and SO_4 for PO_4 groups in the apatite structure; ellestadite, the end member. Am. Mineral. 22:977–986.

Ming, D.W., D.J. Barta, D.C. Golden, C. Galindo, Jr., and D.L. Henninger. 1995. Zeoponic plant growth substrates for space applications. p. 505–515. *In* D.W. Ming and F.A. Mumpton (ed.) Natural zeolites '93: Occurrence, properties, use. International Committee on Natural zeolites. Brockport, NY.

Ming, D.W., and D.C. Golden. 1995. Active synthetic soil. U.S. Patent 5 433 766. Date issued: 19 Sept. 1995.

Mittlefehldt, D.W., and M.M. Lindstrom. 1993. Geochemistry and petrology of a suite of ten Yamato HED meteorites. Proc. Natl. Inst. Polar Res. (Japan) Symp. Antarctic Meteorites. 6:268–292.

Olson, S.R., and R.S. Watanabe. 1957. A method for determining phosphorus absorption maximum for soils as measured by the Langmuir isotherm. Proc. Soil Sci. Soc. Am. 21:144–149.

Resseler, H., and W. Werner. 1989. Preparation and use of ^{33}P labeled carbonate fluorapatite in studies on the effect of phosphate rock containing fertilizers. Z. Pflanzernernahr. Bodenkd. 152:325–332.

Schulze, D.G. 1982. The identification of iron oxides by differential X-ray diffraction and the influence of Al-substitution on the structure of goethite. Ph.D. Thesis, Lehrstuhl fur bodenkunde der Techniche Universitat Munchen, Weihenstephan.

Simpson, D.R. 1968. Substitution in apatite. I. Potassium bearing apatite. Am. Mineral. 53:432–444.

Sommerhauser, J., and K. Katz-Lehnert. 1985. A new partial substitution mechanism of CO_3^{2}/CO_3OH^{3-} and SiO_4^{4-} for the PO_4^{3-} group in hydroxyapatite from the Kaiserstuhl alkaline complexes (SW-Germany). Contrib. Mineral. Petrol. 91:360–368.

Syers, J.K., and A.D. Mackay. 1980. Reactions of Sechura phosphate rock and single superphosphate in soil. Soil Sci. Soc. Am. J. 50: 480–485.

White, R.E., M. Hedley, N. Bolan, and P. Gregg. 1989. Recent developments in the use of phosphate fertilizers on New Zealand pastures. Agric. Sci. (Melbourne) 2:26–32.

Zussman, J. 1977. X-ray diffraction. p. 391–471. *In* J. Zussman (ed.) Physical methods in determinative mineralogy. Academic Press, New York.